SEMARAK ILMU PUBLISHING

Journal of Advanced Research in Fluid Mechanics and Thermal Sciences

Journal homepage:
https://semarakilmu.com.my/journals/index.php/fluid_mechanics_thermal_sciences/index
ISSN: 2289-7879

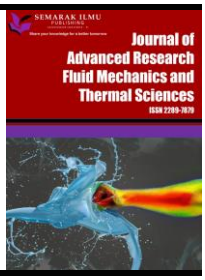

MHD Boundary Layer Flow due to an Exponentially Stretching Surface Through Porous Medium with Radiation Effect and Chemical Reaction

Ahmed Ayesh[1], Faisal Salah[1,*]

[1] Department of Mathematics, College of Science & Arts, King Abdulaziz University, Rabigh 21911, Saudi Arabia

ARTICLE INFO

Article history:
Received 20 May 2023
Received in revised form 23 July 2023
Accepted 1 August 2023
Available online 17 August 2023

Keywords:
MHD stretching sheet; chemical reaction; SLM; thermal radiation

ABSTRACT

In this study, the numerical solutions for an exponentially stretching sheet with radiation effects, chemical reaction and a heat sink is obtained for the problem of MHD boundary layer flow. By using similarity transformation, the PDEs ruling system is converted into an ODEs system. The resulting nonlinear equations governing the flow problem are numerically solved by a successive linearization method (SLM) using MATLAB software. The significance of this paper is to show and compare the results of solving velocity, temperature, and concentration equations in the existence of M changes through SLM for presenting it as appropriate and accurate method for solving nonlinear differential equations. Tables with the numerical data are created for comparison and displayed graphically. Analysis and studies of the effects of different parameters are conducted. The numerical values for the local skin friction coefficient, local Sherwood number, and local Nusselt number are tabulated and explained. The study demonstrates that different parameters have a substantial impact on the fluid flow profiles. It was noted that the concentration patterns were impacted by the reaction rate parameter. In addition, it was found that as the magnetic and radiation parameters increase in value, the local heat transfer rate at the surface decreases.

1. Introduction

Most cosmic events in science, physics, and geometry occurrences that occur in our everyday lives and are described by nonlinear equations. So, it is harder to solve these equations because of these nonlinearities. Some of these nonlinear equations can be approximated mathematically and analytically solved using techniques like the Homotopy (HAM) analysis method proposed by Liao [1], the Homotopy Perturbation (HPM) method discovered by the mathematician He [2], and the Adomain decomposition method (ADM) [3]. Some of these equations can be resolved using traditional numerical techniques like the Keller box, Runge-Kutta, and finite difference methods.

Due to their nonlinearity, the majority of equations that explain how nature behaves lack an accurate analytical solution. However, numerical and semi-analytical techniques can be used to approximate the solutions. However, a novel semi-analytical method for solving non-linear

* *Corresponding author.*
E-mail address: frashed@kau.edu.sa

https://doi.org/10.37934/arfmts.108.2.4861

differential equations is developed as a result of non-analytic solutions of numerical results and difficulties with every existing semi-analytical method. This innovative mathematical technique, known as the "Hybrid Analytical and Numerical Method" or "HAN method," creates an analytical expression from the outcomes of a numerical solution. The analytical formula is a polynomial, and any method may be used to generate the numerical results. The effects of a few physical characteristics have been shown. The applied technique's accuracy and effectiveness have also been demonstrated. The explanation of the hybrid analytical and numerical method and its use in solving a nonlinear heat and mass transfer issue make up the majority of this paper's uniqueness [4-7].

Recent investigations have demonstrated a novel Many non-linear problems in science and engineering have been successfully solved using this approach, including MHD flows of non-Newtonian fluids and transfer over a stretching sheet [8], convective thermal transfer heat to the

MHD boundary layer with a pressure gradient, and others [9,10]. So, this approach has demonstrated extremely high SLM flexibility, accuracy, and efficiency in solving nonlinear equations. technique known as the successive linearization method (SLM).

The boundary layer theory that Ludwig Prandtl put forth in 1904 revolutionized our knowledge of fluid mechanics. In his theory of thin airfoils, Prandtl used the boundary layer idea, making it feasible to calculate the properties of airfoils in practice [11].

Many controlled and natural flows, such as those involved in heating, pumping, and stirring, are influenced by magnetic fields. The relationship between fluid movement and magnetic fields is known as magnetohydrodynamics (MHD), and the fluid in question must be both an electrical conductor and have non-magnetic properties, such as liquid metals, hot ionized gases (plasma), and strong electrolytes. Ishak [12], Seini and Makinde [13] and others examined the heat transmission on the flow of MHD boundary layer over a stretching plate, they discovered that the fluid flow velocity decreases as the magnetic field parameter rises. This is brought on by the existence of the Lorentz force, a resistive force that slows down fluid motion [14]. Numerous academics have studied magnetohydrodynamics (MHD) and flow in porous media over the past ten years. The usage of flow in porous media under the influence of a magnetic field is actually quite beneficial. It is used, among other things, to explore the movement of water, oil, or natural gas in reservoirs in petroleum engineering, the filtration and purification process in chemical engineering, and the investigation of underground water in agricultural engineering. Numerous scholars have researched MHD flow in a porous media with different configurations because of the aforementioned applications; the current work likewise aims to add to this body of knowledge [15-23].

Chemical reactions play a significant role in numerous manufacturing processes, including hot rolling, chemical coating of flat plates, and polymer extrusion. It is impossible for there to be pure water or air in nature because there may be remote mass present. As a result, those combinations could trigger chemical reactions inside the substances. According to Sinha [19], who investigated the impacts of chemical reaction past a permeable plate under sloping temperature and the unsteady MHD free convective flow, reaction rate increases as chemical reaction parameters are increased.

For the MHD flow past an exponentially stretching sheet, Chaudhary *et al.,* [14] and Ishak [12] consider the radiation impacts. The rate of heat transmission increases as the Prandtl number rises, but it decreases as the radiation and magnetic parameters rise. As the radiation parameter grows, the temperature rises. It is crucial to conduct research on MHD flow that considers both the effects of radiation and chemical reactions, particularly in manufacturing sectors. According to Seini and Makinde's [13] study of the MHD boundary layer flow on an exponentially stretching sheet subjected to radiation and chemical reaction, the boundary layer's concentration rises as the reaction rate parameter grows. The findings show that the heat production and reaction rates have a significant impact on the mass and heat transfer rates.

The purpose of this study is to apply the findings of Ishak [12], Khalili *et al.,* [24], and Swain *et al.,* [25] to a more general issue, such as the impact of viscus fluid dissipation and chemical reaction on MHD in porous medium by utilizing SLM technique. In this work, the impacts of various flow parameters found in the governing equations are graphically displayed and tabulated. The more computationally effective SLM method is used to numerically address the issue. The relevant findings are graphically presented and quantitatively discussed.

This article discusses the governing equations for the heat and mass transfer issues on MHD boundary layer flow over a stretching sheet with a heat sink under the influence of chemical reaction and radiation. In this research, continuity, momentum, energy, and concentration equations govern the boundary layer. The boundary layer issues' governing system of PDEs is converted into a system of ODEs using similarity transformation. The system is then solved numerically using the (SLM) approach included in the MATLAB program.

2. Mathematical Formulation of the Problem

2.1 Flow Analysis

Consider a stretched sheet that creates a continuous, two-dimensional flow of an incompressible, viscous, and electrically conducting fluid in a quiescent, uniform-temperature environment, as shown in Figure1. As is appropriate for MHD flow at low magnetic Reynolds numbers, we assume that a variable magnetic field $B(x)$ is applied normal to the sheet and that the induced magnetic field is omitted then $(B(x) = B_0)$. The following equations govern the flow and heat transfer with radiation effects under the standard boundary layer assumption [24,25]:

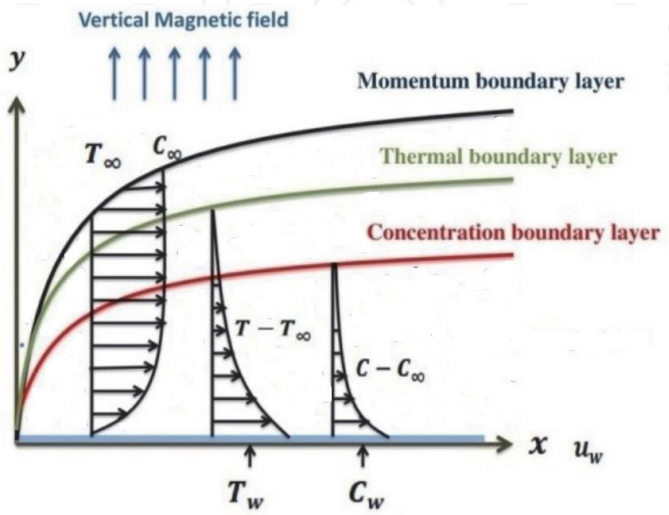

Fig. 1. Physical model of the problem

$$\frac{\partial u}{\partial x} + \frac{\partial v}{\partial y} = 0 \tag{1}$$

$$u\frac{\partial u}{\partial x} + v\frac{\partial u}{\partial y} = \nu\frac{\partial^2 u}{\partial y^2} - \frac{\nu}{k}u - \frac{\sigma}{\rho}B_0^2 u \tag{2}$$

$$u\frac{\partial T}{\partial x} + v\frac{\partial T}{\partial y} = \alpha\frac{\partial^2 T}{\partial y^2} + \frac{1}{\rho c_\rho}\frac{\partial q_r}{\partial y} \tag{3}$$

$$u\frac{\partial C}{\partial x}+v\frac{\partial C}{\partial y}=D\frac{\partial^2 C}{\partial y^2}+K_1(C-C_\infty) \tag{4}$$

where (u, v) are the velocities in the x- and y-directions, respectively, v the kinematic viscosity, ρ is the fluid density, k the thermal conductivity, T the fluid temperature in the boundary layer, c_p the specific heat, C is the boundary layer fluid concentration, D is the mass diffusivity coefficient and q_r is the radiative heat flux. The boundary conditions are given by [24,25]:

$$\begin{gathered}u=U_w=U_0e^{\frac{x}{L}},v=0,T=T_w=T_\infty+T_0e^{\frac{x}{2L}},C=C_w=C_\infty+C_0e^{\frac{x}{2L}},at\ y=0,\\ u\longrightarrow 0,T\longrightarrow T_\infty,C\longrightarrow C_\infty,as\ \ y\longrightarrow\infty\end{gathered} \tag{5}$$

where U_0 is the reference velocity, T_0 the reference temperature and L is the reference length. The development of justifiable simplifications takes up most of the effort in comprehending fluid radiation [22]. One of these simplifications was made by Bataller [23], who presupposed that the fluid is in the optically thin limit and, as a result, that it solely absorbs radiation that is emitted by the boundaries and does not emit any radiation of its own. The problem becomes challenging for an optically thick gas as the gas self-absorption increases.

However, the problem can be simplified by using the Rosseland approximation which simplifies the radiative heat flux as [24]:

$$q_r=-\frac{4\sigma^*}{3k^*}\frac{\partial T^4}{\partial y} \tag{6}$$

where $\sigma^*$and k^* are the Stefan-Boltzmann constant and the mean absorption coefficient, respectively. This approximation only works for intense absorption, which is for an optically thick boundary layer, and is valid at optically far positions from the boundary surface [24,25]. It is believed that the temperature variations within the flow allow for a linear expression of the quantity T^4 as a function of temperature. Hence, expanding T^4 in a Taylor series about T_∞ and neglecting higher-order terms gives

$$T^4\approx 4T_\infty^3-3T_\infty^4 \tag{7}$$

Using Eq. (5) and Eq. (6), Eq. (3) will become:

$$u\ \frac{\partial T}{\partial x}+v\frac{\partial T}{\partial y}=\frac{k}{\rho c_\rho}\frac{\partial^2 T}{\partial y^2}+\frac{16\sigma^*T_\infty^3}{3\rho c_\rho k^*}\frac{\partial^2 T}{\partial y^2} \tag{8}$$

It results from that:

$$B(x)=B_0e^{\frac{x}{2L}} \tag{9}$$

Where B_0 is the constant magnetic field.

2.2 Transformation

The following transformation can be used to convert the momentum and energy equations into the equivalent ordinary differential equations:

$$u = U_0 e^{\frac{x}{L}} f'(\eta), v = -\sqrt{\frac{\nu U_0}{2L}} e^{\frac{x}{2L}} \left(f(\eta) + \eta f'(\eta)\right)$$
$$T = T_\infty + T_0 e^{\frac{x}{2L}} \theta(\eta), \ \ \eta = \sqrt{\frac{U_0}{2\nu L}} \ \ e^{\frac{x}{2L}} y, \tag{10}$$

where $f(\eta)$ is the dimensionless stream function, $\theta(\eta)$ is the dimensionless temperature, $\phi(\eta)$is the dimensionless concentration and primes signify differentiation with regard to η. η is the similarity variable. Ordinary differential equations that have been altered are:

$$f''' + ff'' - 2f'^2 - (M + B)f' = 0, \tag{11}$$

$$\left(1 + \frac{4}{3}K\right)\theta'' + Pr(f\theta' - f'\theta) = 0, \tag{12}$$

$$\phi'' + S_c(f\phi' - f'\phi - \gamma\phi) = 0 \tag{13}$$

where $K = \frac{4\sigma^* T_\infty^3}{k^* k}$ the radiation parameter, $M = \frac{2\sigma B_0^2 L}{U_0 \rho} e^{\frac{x}{L}}$ is the magnetic parameter, $S_c = \frac{\nu}{D}$ is Schmidt number, $\gamma = \frac{2LK_R}{U_w}$ and $P_r = \frac{\rho \nu C_\rho}{k}$ is the Prandtl number. The modified border conditions are:

$$f(0) = 0, f'(0) = 1, \theta(0) = 1, \phi(0) = 1$$
$$f'(\eta) \to 0, \theta(\eta) \to 0, \phi(\eta) \to 0 \ as \ \eta \to \infty. \tag{14}$$

3. Solution of the Problem

3.1 Procedure of computational

Here successive linearization method (SLM) is implemented to obtain the numerical solutions for nonlinear systems in Eq. (11) to Eq. (13) corresponding to the boundary condition in Eq. (14) [8,9,26]. For SLM solution we select the initial guesses functions $f(\eta)$ and $\theta(\eta)$ in the form,

$$f(\eta) = f_i(\eta) + \sum_{m=0}^{i-1} F_m(\eta),$$
$$\theta(\eta) = \theta_i(\eta) + \sum_{m=0}^{i-1} \theta_m(\eta), \tag{15}$$
$$\phi(\eta) = \phi_i(\eta) + \sum_{m=0}^{i-1} \phi_m(\eta)$$

here, the functions $\theta(\eta)$, $f_i(\eta)$ and $\phi(\eta)$are representative of unknown functions. $F_m(\eta), m \geq 1$, $\theta_m(\eta), m \geq 1$, $\phi_m(\eta), m \geq 1$ are a successive approximation, which are obtained by recursively solving the linear part of the equation that results from substituting Eq. (13) in the governing equations. The mean idea of SLM that the assumption of unknown function $f_i(\eta)$, $\theta_i(\eta)$ and $\phi_i(\eta)$are very small when i becomes larger, therefore, the nonlinear terms in $f_i(\eta)$, $\theta_i(\eta)$ and their derivatives are considered to be smaller and thus neglected. The intimal guess functions$f_0(\eta)$, $\theta_0(\eta)$, $\phi_i(\eta)$which are selected to satisfy the boundary conditions,

$$F(0) = 0, F_0'(0) = 1, \theta(0) = 1, \phi(0) = 1$$
$$F'(\eta) \to 0, \theta(\eta) \to 0, \phi(\eta) \to 0 \ as \ \eta \to \infty \tag{16}$$

which are taken to be in the form,

$$F_0(\eta) = I - e^{-\eta}, \quad F_0{}' = e^{-\eta}$$
$$F_0(0) = 0, \theta = e^{-\eta}, \phi = e^{-\eta} \tag{17}$$

The succeeding solutions f_i and θ_i are then computed starting from the first guess by solving the linearized from equation, which is obtained by inserting Eq. (15) in the governing Eq. (11) to Eq. (13). The linearized equations that must be solved are as follows:

$$f_i''' + a_{1,i-1} f_i'' + a_{2,i-1} f_i' + a_{3,i-1} f_i = r_{1,i-1} \tag{18}$$

$$A\theta_i'' + b_{1,i-1}\theta_i' + b_{2,i-1}\theta_i + a_{4,i-1} f_i' + a_{5,i-1} f_i = r_{2,i-1}, \tag{19}$$

$$\phi_i'' + S_c\left[a_{6,i-1} f_i + c_{1,i-1}\phi_i' - a_{7,i-1} f_i' - c_{2,i-1}\phi_i - \gamma\phi_i\right] = r_{3,i-1}, \tag{20}$$

where,

$$a_{1,i-1} = \sum_{m=0}^{i-1} F_m,\ a_{2,i-1} = -4\left[\sum_{m=0}^{i-1} F'_m + (M+B)\right],\ a_{3,i-1} = \sum_{m=0}^{i-1} F''_m,$$

$$a_{4,i-1} = P_r \sum_{m=0}^{i-1} F'_m,\ a_{5,i-1} = P_r \sum_{m=0}^{i-1} \theta'_m,\ a_{6,i-1} = S_c \sum_{m=0}^{i-1} \phi'_m,\ a_{7,i-1} = S_c \sum_{m=0}^{i-1} \phi_m$$

and,

$$r_{1,i-1} = -\sum_{m=0}^{i-1} F'''_m - \sum_{m=0}^{i-1} F_m \sum_{m=0}^{i-1} F''_m + 2\left(\sum_{m=0}^{i-1} F'_m\right)^2 + (M+B)\sum_{m=0}^{i-1} F'_m,$$

$$b_{1,i-1} = P_r \sum_{m=0}^{i-1} F_m,\ b_{2,i-1} = P_r \sum_{m=0}^{i-1} F'_m,$$

$$r_{2,i-1} = -A\sum_{m=0}^{i-1} \theta''_m - P_r \sum_{m=0}^{i-1} F_m \sum_{m=0}^{i-1} \theta'_m + P_r \sum_{m=0}^{i-1} F'_m \sum_{m=0}^{i-1} \theta_m,$$

and,

$$c_{1,i-1} = S_c \sum_{m=0}^{i-1} F_m\,, c_{2,i-1} = -S_c\left(\sum_{m=0}^{i-1} F'_m + \gamma\right),$$

$$r_{3,i-1} = -\sum_{m=0}^{i-1} \phi''_m - S_c \sum_{m=0}^{i-1} F_m \sum_{m=0}^{i-1} \phi'_m + S_c \sum_{m=0}^{i-1} F'_m \sum_{m=0}^{i-1} \phi_m + \gamma S_c \sum_{m=0}^{i-1} \phi_m.$$

The answer for f_i, θ_i and ϕ_i has been found when we solve Eq. (8) and Eq. (10) iteratively, and finally, after K iterations, the result $f(\eta)$ and $\theta(\eta)$ may be represented as:

$$\sum_{m=0}^{K} F_m(\eta), \theta(\eta) = \sum_{m=0}^{K} \theta_m(\eta)\,, \phi(\eta) = \sum_{m=0}^{K} \phi_m(\eta)\,, \tag{21}$$

First, change the domain solution from $[0, \infty)$ to $[-1,1]$ in order to apply SLM. On the Chebyshev spectral collection method, SLM is based. This approach is based on the Chebyshev polynomials with interval $[-1,1]$. As a result, utilizing the truncation of the domain technique the issue is resolved in the range $[0, L]$, where L is a scaling parameter that is utilized to impose the boundary condition at infinity. Thus, this can be acquired by the transition

$$\frac{\eta}{L} = \frac{\xi+1}{2}, \qquad -1 \le \xi \le 1 \tag{22}$$

From Gauss-Lobatto collocation points, we can discretize the domain [−1,1] as follows:

$$\xi = cos\frac{\pi j}{N}, \quad F_i \approx \sum_{k=0}^{N} F_i(\xi_k)T(\xi_j), \quad j = 0,1,\dots,N \tag{23}$$

where, N is the number of collection points and $T_k$is the k^{th} Chebyshev polynomial given by$T_k(\xi) = \cos\left[kcos^{-1}(\xi)\right]$.

The derivatives of the variable at the collocation points are in the form:

$$\begin{aligned}\frac{d^{\,r}F_i}{d\eta^r} &= \sum_{k=o}^{N} D_{k_j}^r F_i(\xi_k), \quad j = 0,1,\dots,N,\\ \frac{d^{\,r}\theta_i}{d\eta^r} &= \sum_{k=o}^{N} D_{k_j}^r \theta_i(\xi_k), \quad j = 0,1,\dots,N,\end{aligned} \tag{24}$$

where r is the differentiation order and$D = \frac{2}{L}D$. The matrix of Chebyshev spectral differentiation is D.

We arrive at the matrix equation by substituting Eq. (22) through Eq. (24) into Eq. (18) to Eq. (20).

$$A_{i-1}X_i = R_{i-1,} \tag{25}$$

where,

$$\begin{aligned}&A_{i-1} = \begin{bmatrix}A_{11} & A_{12} & A_{13}\\ A_{21} & A_{22} & A_{23}\\ A_{31} & A_{32} & A_{33}\end{bmatrix}, \quad X_{i-1} = \begin{bmatrix}F_i\\ \theta_i\\ \phi_i\end{bmatrix}, \quad R_{i-1} = \begin{bmatrix}r_{1,i-1}\\ r_{2,i-1}\\ r_{3,i-1}\end{bmatrix},\\ &A_{11} = D^3 + a_{1,i-1}D^2 + a_{2,i-1}D + a_{3,i-1}I, A_{12} = 0, A_{13} = 0\\ &A_{21} = a_{4,i-1}D + a_{5,i-1}I\\ &A_{22} = AD^2 + b_{1,i-1}D + b_{2,i-1}I\\ &A_{23} = 0,\\ &A_{31} = a_6 I - a_7 D,\\ &A_{32} = 0, A_{33} = D^2 + c_1 D + c_2 I\end{aligned} \tag{26}$$

By using the method described above, we can get the solution as $X_i = {A_{(i-1)}}^{-1}R_{i-1}$.

3.2 Convergence Analysis

The convergence for numerical of $-f''(0)$ for different order of approximation when $M = 1$, $B = 0.1$, $P_r = 1\ and\ K = 1$ is shown in Table 1.

Table 1
The convergence for numerical values of $-f''(0)$ for different order of approximation when, $M = 1, B = 0.01$, $P_r = 1, S_c = 0.22$, $\gamma = 1$ *and* $K = 1$

Order of approximation	$-f''(0)$	$-\theta'(0)$	$-\phi'(0)$
0	1.615101602	0.505885364	1.574608168
1	1.632142667	0.451872939	0.620492553
2	1.632261331	0.449949006	0.601321390
3	1.632261349	0.449947464	0.599997716
5	1.632261349	0.449947464	0.599997446
10	1.632261349	0.449947464	0.599997446
15	1.632261349	0.449947464	0.599997446
25	1.632261349	0.449947464	0.599997446
30	1.632261349	0.449947464	0.599997446
35	1.632261349	0.449947464	0.599997446
40	1.632261349	0.449947464	0.599997446
50	1.632261349	0.449947464	0.599997446

4. Results and Discussion

4.1 Validation of Study

Table 2, where $K = 1, P_r = 1, \gamma = 1$ and $S_c = 0.22$, shows the Nusselt number $-\theta'(0)$ values for various radiation parameters. The remaining parameters are set to zero. The table illustrates the agreement between the results by comparing them to those of Khalili *et al.,* [24]. The values of the Skin Friction Coefficient and Local Sherwood Number are shown in Table 2 and Table 5, respectively, for various values of the contributing components. The results are in great agreement, as shown in the table comparing the results with those of Khalili *et al.,* [24]

Table 2
Comparison of numerical values of $-f''(0)$ with references [24]

M	K	Pr	Sc	γ	Khalili *et al.,* [24]	Present work
0	1	1	0.22	1	1.281933	1.281808
1	1	1	0.22	1	1.629195	1.629177
2	1	1	0.22	1	1.912633	1.9126203
4	1	1	0.22	1	2.379381	2.379367

In Table 3 the Nusselt number $-\theta'(0)$ values are shown below for various Prandtl number values while the other parameters are set to zero. The comparison between the results obtained and those of [12] is provided in the table, and it is demonstrated that the results accord with one another.

Table 3
Comparison of numerical values of $-\theta'(0)$ with Ishak [12]

K	M	Pr	Ishak [12]	Present work
0	0	1	-0.9548	-0.95478
0	0	2	-1.4715	-1.47146
0	0	3	-1.8691	-1.86907
0	0	5	-2.5001	-2.50013
0	0	10	-3.6604	-3.66037
0	1	1	-0.8611	-0.86109
1	0	1	-0.5312	-0.53118

In Table 4 the Nusselt number $-\theta'(0)$ values are shown below for various Prandtl number values while the other parameters are set to zero. The comparison between the results obtained and those of [25] is provided in the table, and it is demonstrated that the results accord with one another.

Table 4
Comparison of numerical values of $-\theta'(0)$ with Swain *et al.,* [25]

M	B	S	Pr	Kp	Swain *et al.,* [25]	Present work
0	0	0	1	100	0.53119	0.53116
0	0	0	2	100	1.41751	1.41746
0	0	0	1	100	0.9547	0.95478

In Table 5 the Sherwood number $-\phi'(0)$ values are shown below for various Prandtl number values while the other parameters are set to zero where $K = 1, P_r = 1, \gamma = 1 \text{ and } S_c = 0.22$.

The comparison between the results obtained and those of Khalili *et al.,* [24] is provided in the table, and it is demonstrated that the results accord with one another.

Table 5
Comparison of numerical values of $-\phi'(0)$ with Khalili *et al.,* [24]

M	K	Pr	Sc	γ	Khalili *et al.,* [24]	Present work
0	1	1	0.22	1	0.621791	0.621762
1	1	1	0.22	1	0.600183	0.600159
2	1	1	0.22	1	0.586782	0.586776
4	1	1	0.22	1	0.569903	0.569901

4.2 Results

The effects of magnetic parameter on velocity, temperature and concentration profiles are shown in Figure 2, Figure 3 and Figure 4 accordingly. Figure 2 demonstrates how velocity decreases as M rises. It has been demonstrated that the magnetic parameter M lowers fluid velocity. The magnetic field's presence, which opposes the flow, slows the fluid down. This is related to the Lorentz force, a resistive force that develops as a result of applying a transverse magnetic field to an electric-conducting fluid. Skin friction coefficient rises as M rises (Table 6). As a result, the fluid's velocity is increased and decreased by the shear wall tension. The fluid's temperature and concentration then rise as M increases in Figure 3 and Figure 4. The fluid is heated by the magnetic field that is being applied, increasing the temperature.

The graph in Figure 5 shows that as the permeability parameter grows, the fluid flow resistance force decreases, i.e., as the permeability parameter grows, the fluid flow velocity grows. The impact of the permeability B parameter on temperature profiles is depicted in Figure 6. The temperature profile is shown to be decreasing in Figure 6 as a result of an increase in the porosity parameter. Figure 7 displays how the permeability B parameter affects dimensionless concentration. The concentration profile is shown to decline as the permeability B parameter increases.

Figure 8 illustrates how the fluid's temperature is impacted by the Prandtl number. The temperature is lowered as Pr increases. Higher Prandtl numbers suggest that the fluid has smaller boundary layer structures and lower thermal conductivity [20]. As a result, the thermal barrier layer is thinner, allowing heat to escape the sheet more quickly. Table 2 demonstrates that as Pr rises, the local Nusselt number rises, which suggests that the rate of heat exchanges rises. As a result, heat radiates from the sheet more quickly, and the temperature drops.

Figure 9 demonstrates that a decrease in concentration has resulted from an increase in the Schmidt number. The mass diffusivity is inversely correlated to the Schmidt number. This explains why the boundary layer concentration thins out as Sc increases.

Figure 10 shows how the radiation parameter K affects the temperature profile. When the radiation parameter is greater, the temperature drops because the increased thermal radiation creates a greater convection moment at the boundary. As demonstrated in Table 6, the local Nusselt number falls as K rises. The boundary layer's temperature rises as the rate of heat transmission decreases. The reaction rate parameter measures how quickly a reactant or a product reacts in a certain reaction. Figure 11 illustrates the impact on the concentration profile caused by a change in the reaction rate parameter γ, where the concentration drops as the parameter γ is increased. This is due to the fact that the concentration boundary layer thickens with increasing reaction rate.

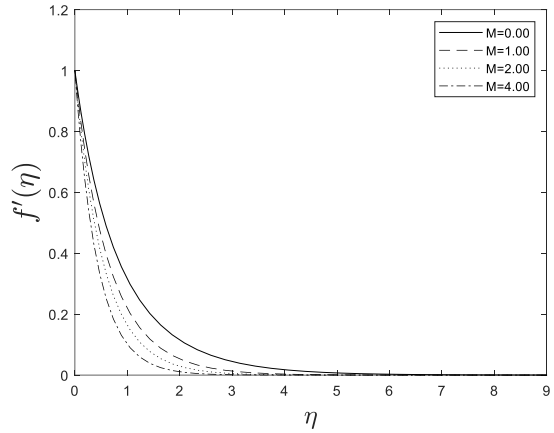

Fig. 2. Velocity profiles for different values of M when Pr=1 and K=1

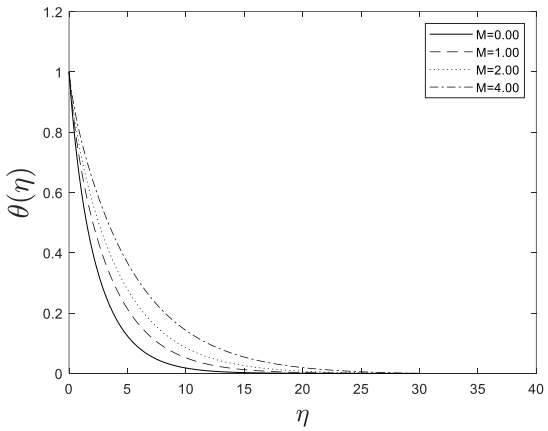

Fig. 3. Temperature profiles for different values of M when Pr=1 and K=1

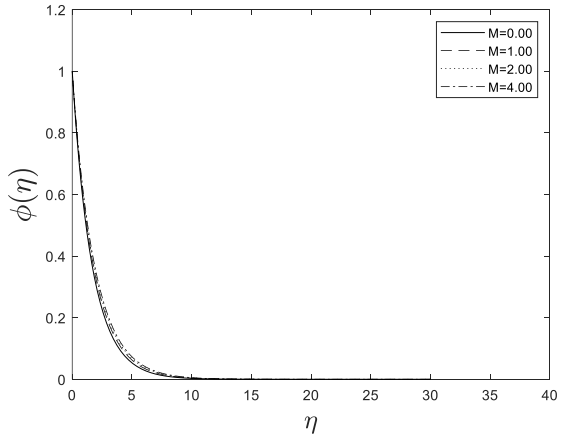

Fig. 4. Concentration profiles for different values of M when Pr=1 and K=1

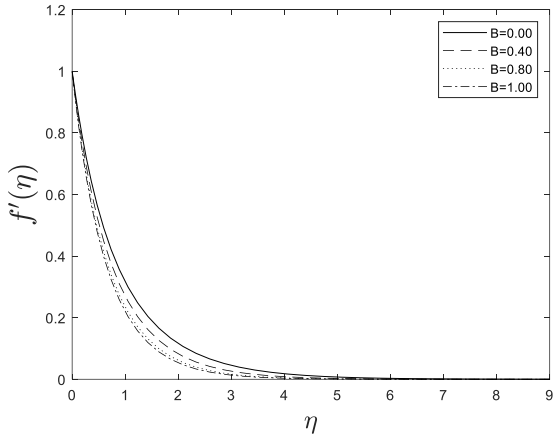

Fig. 5. Velocity profiles for different values of B when Pr =1 and K=1

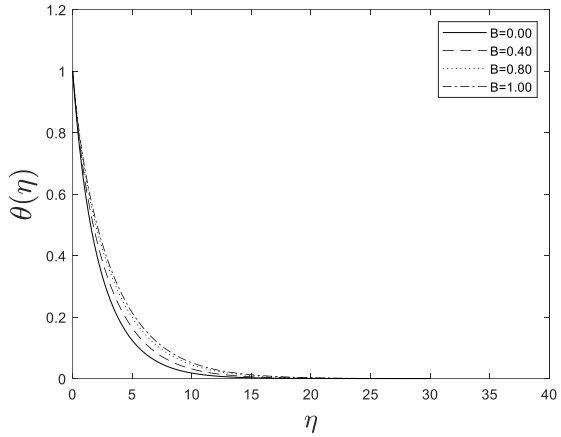

Fig. 6. Temperature profiles for different values of B when Pr=1 and K=1

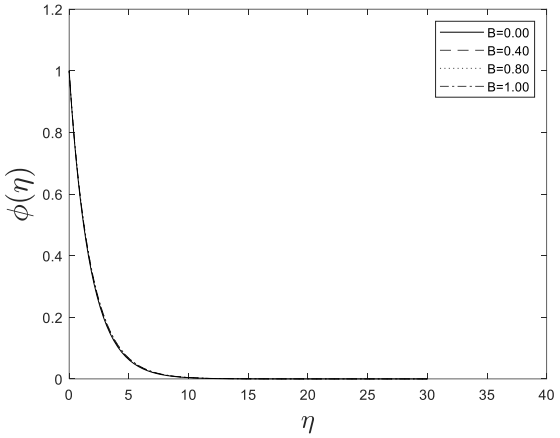

Fig. 7. Concentration profiles for different values of B when Pr=1 and K=1

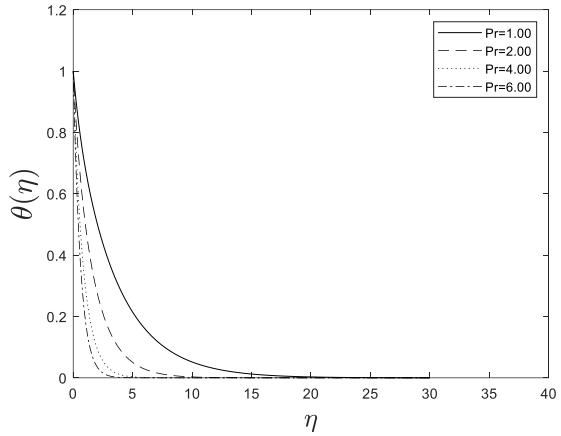

Fig. 8. Temperature with Prandti number P_r variation when $M = 1, S_c = 0.22$ and $K = 1$

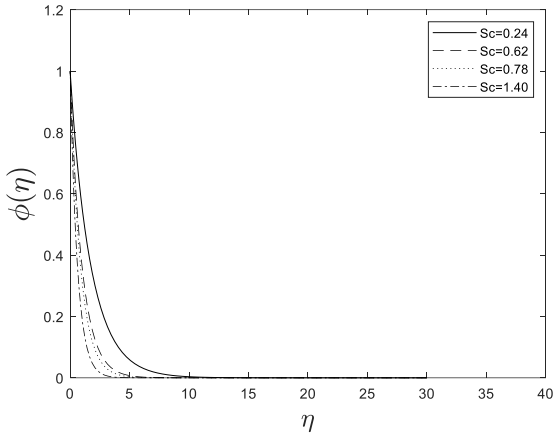

Fig. 9. Concentration profiles for different values of S_c when $P_r = 1, \mathrm{M} = 2$ and $K = 1$

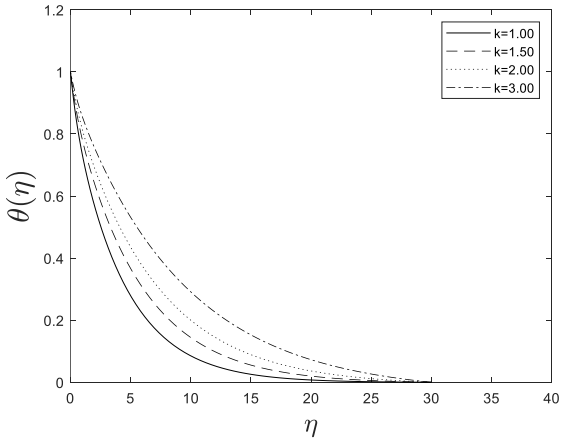

Fig. 10. Temperature profiles for different values of K when Pr=1 and M=1

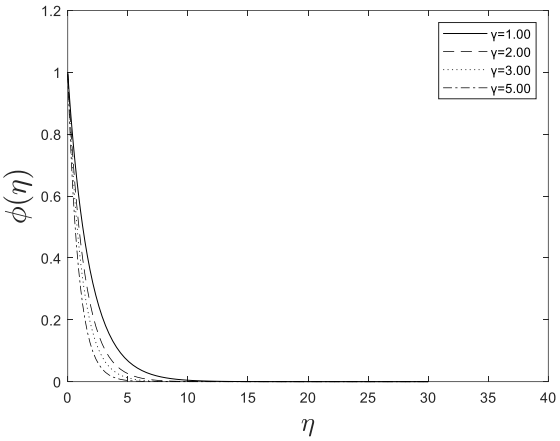

Fig. 11. Concentration profiles for different values of γ when Pr = 1, M=2 and K=1

Table 6
The Skin Friction Coefficient, Nusselt number, and Sherwood number for various values of parameters

M	P_r	B	S_c	K	γ	$\lvert f'(0)\rvert$	$-\theta'(0)$	$-\phi'(0)$
0	1	0.01	0.22	1	1	1.285790	0.530097	0.621468
1						1.632261	0.449947	0.599997
2						1.915239	0.398416	0.586665
4						2.381469	0.333404	0.569836
1		0.01	0.22	1	1	1.632261	0.449947	0.599997
						1.632261	0.769486	0.599997
						1.632261	1.025950	0.599997
						1.632261	1.244854	0.599997
1	1	0.02	0.22	1	1	1.635338	0.449326	0.599835
		0.10				1.659748	0.444455	0.598567
1	1	0.01	0.24	1	1	1.632261	0.449947	0.630134
			0.62			1.632261	0.449947	1.073205
1	1	0.01	0.22	2	1	1.632261	0.308319	0.599997
				3		1.632261	0.236329	0.599997
1	1	0.01	0.22	1	3	1.632261	0.449947	0.914789
					5	1.632261	0.449947	1.137956

5. Concluding Remarks

In this study, we investigated the MHD boundary layer flow due to an exponentially stretching surface through a porous medium with radiation effect and chemical reaction. The governing equations were transformed into a dimensionless form using appropriate scaling parameters, and similarity transformations were introduced to reduce the PDEs to a set of ODEs. The transformed ODEs were solved numerically using (SLM) method.

The effects of various parameters on the velocity, temperature, and concentration profiles were investigated. It was found that the velocity profile decreases with an increase in the magnetic field strength and increases with an increase in the porous medium permeability. The temperature profile increases with an increase in the radiation parameter, and the concentration profile decreases with an increase in the chemical reaction parameter. The Skin Friction Coefficient, Nusselt number, and Sherwood number were analyzed and found to be influenced by the magnetic field strength, porous medium permeability, radiation parameter, and chemical reaction parameter. The present results were compared with the work of other authors in the field, showing good agreement. This study provides valuable insights into the MHD boundary layer flow due to an exponentially stretching surface through a porous medium with radiation and chemical reaction effects, which can be beneficial for various practical applications. In future we can extend this problem for another class of non-Newtonian fluids namely rate type fluids in three dimensional with slip conditions.

Acknowledgement
This research was not funded by any grant.

References
[1] Liao, Shi-Jun. "The proposed homotopy analysis technique for the solution of nonlinear problems." PhD diss., PhD thesis, Shanghai Jiao Tong University, 1992.
[2] He, Ji-Huan. "Homotopy perturbation technique." *Computer methods in applied mechanics and engineering* 178, no. 3-4 (1999): 257-262. https://doi.org/10.1016/S0045-7825(99)00018-3
[3] Esmaili, Q., A. Ramiar, E. Alizadeh, and D. D. Ganji. "An approximation of the analytical solution of the Jeffery–Hamel flow by decomposition method." *Physics Letters A* 372, no. 19 (2008): 3434-3439.

https://doi.org/10.1016/j.physleta.2008.02.006
[4] Jalili, Payam, Hossein Narimisa, Bahram Jalili, and D. D. Ganji. "Micro-polar nanofluid in the presence of thermophoresis, hall currents, and Brownian motion in a rotating system." *Modern Physics Letters B* 37, no. 01 (2023): 2250197. https://doi.org/10.1142/S0217984922501974
[5] Jalili, Payam, Hossein Narimisa, Bahram Jalili, Amirali Shateri, and D. D. Ganji. "A novel analytical approach to micro-polar nanofluid thermal analysis in the presence of thermophoresis, Brownian motion and Hall currents." *Soft Computing* 27, no. 2 (2023): 677-689. https://doi.org/10.1007/s00500-022-07643-2
[6] Jalili, Payam, Ali Ahmadi Azar, Bahram Jalili, Zohreh Asadi, and Davood Domiri Ganji. "Heat transfer analysis in cylindrical polar system with magnetic field: a novel hybrid analytical and numerical technique." *Case Studies in Thermal Engineering* 40 (2022): 102524. https://doi.org/10.1016/j.csite.2022.102524
[7] Jalili, Bahram, Amirhossein Rezaeian, Payam Jalili, Davood Domeri Ganji, and Yasir Khan. "Squeezing flow of Casson fluid between two circular plates under the impact of solar radiation." *ZAMM-Journal of Applied Mathematics and Mechanics/Zeitschrift für Angewandte Mathematik und Mechanik* (2023): e202200455. https://doi.org/10.1002/zamm.202200455
[8] Shateyi, S., and S. S. Motsa. "Variable viscosity on magnetohydrodynamic fluid flow and heat transfer over an unsteady stretching surface with Hall effect." *Boundary Value Problems* 2010 (2010): 1-20. https://doi.org/10.1155/2010/257568
[9] Ahmed, Mohammed A. Mohammed, Mohammed E. Mohammed, and Ahmed A. Khidir. "On linearization method to MHD boundary layer convective heat transfer with low pressure gradient." *Propulsion and Power Research* 4, no. 2 (2015): 105-113. https://doi.org/10.1016/j.jppr.2015.04.001
[10] Salah, Faisal, A. K. Alzahrani, Abdelmgid OM Sidahmed, and K. K. Viswanathan. "A note on thin-film flow of Eyring-Powell fluid on the vertically moving belt using successive linearization method." *International Journal of Advanced and Applied Sciences* 6, no. 2 (2019): 17-22. https://doi.org/10.21833/ijaas.2019.02.004
[11] Anderson, John David. *A history of aerodynamics: and its impact on flying machines*. No. 8. Cambridge university press, 1998. https://doi.org/10.1017/CBO9780511607158
[12] Ishak, Anuar. "MHD boundary layer flow due to an exponentially stretching sheet with radiation effect." *Sains Malaysiana* 40, no. 4 (2011): 391-395.
[13] Seini, Y. I., and O. D. Makinde. "MHD boundary layer flow due to exponential stretching surface with radiation and chemical reaction." *Mathematical Problems in Engineering* 2013 (2013). https://doi.org/10.1155/2013/163614
[14] Chaudhary, Santosh, Sawai Singh, and Susheela Chaudhary. "Thermal radiation effects on MHD boundary layer flow over an exponentially stretching surface." *Applied Mathematics* 6, no. 02 (2015): 295. https://doi.org/10.4236/am.2015.62027
[15] Dey, Debasish, O. D. Makinde, and Rupjyoti Borah. "Analysis of dual solutions in MHD fluid flow with heat and mass transfer past an exponentially shrinking/stretching surface in a porous medium." *International Journal of Applied and Computational Mathematics* 8, no. 2 (2022): 66. https://doi.org/10.1007/s40819-022-01268-7
[16] Sulemana, M., I. Y. Seini, and O. D. Makinde. "Hydrodynamic Boundary Layer Flow of Chemically Reactive Fluid over Exponentially Stretching Vertical Surface with Transverse Magnetic Field in Unsteady Porous Medium." *Journal of Applied Mathematics* 2022 (2022). https://doi.org/10.1155/2022/7568695
[17] Etwire, Christian John, Ibrahim Yakubu Seini, Musah RABIU, and Oluwole Daniel Makinde. "Impact of thermophoretic transport of Al2O3 nanoparticles on viscoelastic flow of oil-based nanofluid over a porous exponentially stretching surface with activation energy." *Engineering Transactions* 67, no. 3 (2019): 387-410.
[18] Nayak, Manoj Kumar, Vinay Shankar Pandey, Dharmendra Tripathi, Noreen Sher Akbar, and Oluwole D. Makinde. "3D MHD cross flow over an exponential stretching porous surface." *Heat Transfer* 49, no. 3 (2020): 1256-1280. https://doi.org/10.1002/htj.21661
[19] Sinha, S. "Effect of chemical reaction on an unsteady MHD free convective flow past a porous plate with ramped temperature." In *Proceedings of International Conference on Frontier in Mathematics*, pp. 204-210. 2015.
[20] Aboeldahab, Emad M., and Mahmoud S. El Gendy. "Radiation effect on MHD free-convective flow of a gas past a semi-infinite vertical plate with variable thermophysical properties for high-temperature differences." *Canadian Journal of Physics* 80, no. 12 (2002): 1609-1619. https://doi.org/10.1139/p01-146
[21] Cogley, Allen C., Walter G. Vincent, and Scott E. Gilles. "Differential approximation for radiative transfer in a nongrey gas near equilibrium." *Aiaa Journal* 6, no. 3 (1968): 551-553. https://doi.org/10.2514/3.4538
[22] Xu, Huijin J., Zhanbin B. Xing, F. Q. Wang, and Z. M. Cheng. "Review on heat conduction, heat convection, thermal radiation and phase change heat transfer of nanofluids in porous media: Fundamentals and applications." *Chemical Engineering Science* 195 (2019): 462-483. https://doi.org/10.1016/j.ces.2018.09.045
[23] Bataller, Rafael Cortell. "Similarity solutions for boundary layer flow and heat transfer of a FENE-P fluid with thermal radiation." *Physics Letters A* 372, no. 14 (2008): 2431-2439. https://doi.org/10.1016/j.physleta.2007.11.049
[24] Khalili, Noran Nur Wahida, Abdul Aziz Samson, Ahmad Sukri Abdul Aziz, and Zaileha Md Ali. "Chemical reaction and

radiation effects on MHD flow past an exponentially stretching sheet with heat sink." In *Journal of Physics: Conference Series*, vol. 890, no. 1, p. 012025. IOP Publishing, 2017. https://doi.org/10.1088/1742-6596/890/1/012025

[25] Swain, I., S. R. Mishra, and H. B. Pattanayak. "Flow over exponentially stretching sheet through porous medium with heat source/sink." *Journal of Engineering* 2015 (2015). https://doi.org/10.1155/2015/452592

[26] Sidahmed, Abdelmgid, and Faisal Salah. "Radiation effects on MHD flow of second grade fluid through porous medium past an exponentially stretching sheet with chemical reaction." *Journal of Advanced Research in Fluid Mechanics and Thermal Sciences* 99, no. 2 (2022): 1-16. https://doi.org/10.37934/arfmts.99.2.116